A New Design of Single Side Brushless Direct Current Linear Motor

Mahir Dursun and Ali Saygın
Faculty of Technology, Department of Electrical and Electronics Engineering, Gazi University, Ankara, Turkey
Email: {mdursun, asaygin}@gazi.edu.tr

Semih Özden [1] and Ahmet Fenercioğlu [2]
[1] Electricity and Energy Department, OSTIM Vocational High School, Gazi University, Ankara, Turkey
[2] Dept. of Mechatronics Engineering, Faculty of Engineering and Natural Sciences, Gaziosmanpaşa University, Tokat, Turkey
Email: sozden@gazi.edu.tr, ahmetfenercioglu@gop.edu.tr

***Abstract*—Linear electrical motors are electrical machines which directly convert electrical energy into linear motion without requiring any extra mechanical components. So far, DC and AC linear motors have been employed in many positioning systems. On the other hand, the main reasons of DC linear motors have not been widespread are their stroke limitations and high cost. This paper presents for mechatronic systems a geometric and magnetic design of single-sided, linear brushless direct current motor (LBLDC). The designed motor has 3 A, 24 V, 72 W, and 70 N pull force, high force/volume rated and low cost. Its characteristics were analyzed by using finite-element software. The prototype was simulated and released of a single-sided LBLDC. The obtained results were compared with the results obtained by the analytical methods.**

***Index Terms*—permanent magnet, linear motor, brushless dc motor, motor design**

I. Introduction

To convert electrical energy to mechanical energy electric motors is used. In many industrial systems a linear force is required. On the other hand, to linear motion from a circular electric motor to achieve many additional parts are needed. Also the cost of this process is so high, reliability, position control, and increases the need for maintenance. So, in the industrial applications it is needed to linear motors. A LBLDC motor is an electric machine with a classic three-phase stator like that of an induction motor and the rotor has surface-mounted permanent magnets. The moving part of motor was called as translator and mounted at the surface and stationary part was called rotor. The polarity reversal is performed by power transistors switching in synchronization with the translator position. The LBLDC motor is driven by rectangular voltage strokes coupled with the given translator position. The generated stator flux interacts with the translator flux and defines the force and thus velocity of the motor.

These motors can be used in various applications, such as medical equipment, home appliances, building controls, automotive or industrial applications, and robots…etc. Because of those characteristics: commutation done on windings, high reliability (no brush wear), low EMI, high efficiency, medium construction complexity (multiple fields, delicate magnets), driven by multi-phase inverter controllers. As a result these motors began to spread quickly and are more reliable than the use of linear motors suitable for producing linear motion is direct. Because of these reasons, linear motors are being used in linear movement systems widespread in recent years [1], [2]. Linear DC motors are very small powerful applications, transportation, and missile launch systems encountered in many applications [3].

DC motors it is more advantageous than DC linear motor in this respect of the coil [4], [5] and the magnet [6] as well, operation. DC linear motors because of the disadvantages of the most common problems, due to the brush-collector are made of a single layer. Green and Paul, Basak and Oveshott, Nasar, Basak and Anay have designed in the form of single-layer linear DC motor windings [3]-[10]. Emerging producing NdFeB magnets and easy to control thanks to the more force the use of linear motors, direct current is increasing with each passing day. With these magnets force by the coil motors produced higher flow rate.

BLDC motors, the classic DC motors, often malfunction due to wear and create overheating, switching and brushes are designed to overcome the shortcomings of need, and they require constant maintenance. Switching operation is performed electronically from the brush and collector does not need maintenances at BLDC motor. In recent years, with the development of semiconductor technology and micro-controllers, and material control systems on the basis of the research results improved magnet brushless dc motors industry has gained importance with the development of materials [1]-[10]

Manuscript received February 5, 2014; revised September 15, 2014.

©2015 Engineering and Technology Publishing

doi: 10.12720/joace.3.4.336-342

In this study, the control system is very simple and the force / current one-sided LBLDC motor with a high percentage are designed. In order to increase the force produced and also the armature coils of the armature coils wound multilayer system has been developed to give you energy collector and brushes. Finite element software and analytical methods were analyzed. In both cases, the advantages and characteristics of the motor by comparing the results obtained have been determined.

II. Design of LBLDC

The operating principle of the rotational motor as seen in Fig. 1 is used in with reference to designing an annular electric motor with its own types. As with other linear motor design when designing LBLDC motor determining the parameters is performed and their type can be taken into the working principle of a circular LBLDC.

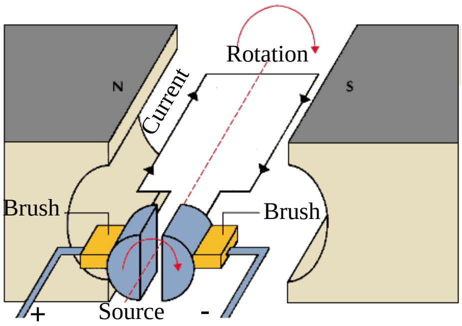

Figure 1. Operating principle of the a circular motor

A. Operating Principle of LBLDC

As shown in Fig. 2 it can exploded LBLDC to rotational BLDC can be considered. The stator of rotational BLDC (the outer stationary part) and the rotor (rotating inner part) because they are intertwined in a circular pattern formed by the rotating field windings in the stator rotation motion [10].

In BLDC first side (Energy is applied to movable part) occurring in the walking area of the coil and the second side (where the fixed part of the permanent magnet), perform a linear movement because of overlap [10].

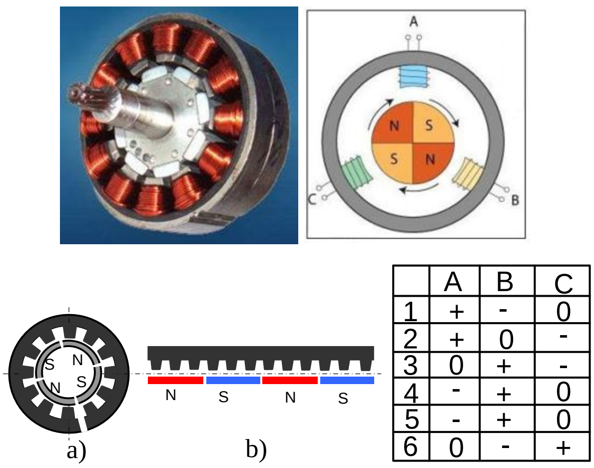

	A	B	C
1	+	-	0
2	+	0	-
3	0	+	-
4	-	+	0
5	-	+	0
6	0	-	+

Figure 2. Transforming from BLDC to LBLDC [10].

B. The Design and Working Principle of the One-Sided Linear Brushless Direct Current Motor

According to the Lorentz law, if a conductor placed in the magnetic field and current is passed through this conductor and induced force is calculated by Equation 1

$$F = I \times L \times B = IBL \sin\theta \tag{1}$$

where F is the induced force at the conductor as (N), I is the current of the conductor (A), L is length of conductor (m), and B is magnetic flux density (Wb/m2). The traditional type of single-layered coils direct current DC linear motors. Brushless are contact to uninsulated conductors where are placed upper layer of the coils for help of energy transferring. If two or more layer is made of the brush system, energy can be given. Therefore generated forces remained at very low levels. Multi-layer designs with complex power electronics circuits and the position of the sensors for switching its needed has been costly for long distances. As a result, linear motors are widespread.

In this study developed the three-dimensional drawing of the LBLDC was given in Fig. 3. One part of motor is moving part. It has 1010 steel core and includes phase's coils. Another part was mounted that includes 40 parts NdFeB magnets and it is stationary part. Translator windings of the motor phases are placed in the slots and power is applied according to the position of the translator. Each phase winding has 30 turns, and conductor diameter is 0.8 mm.

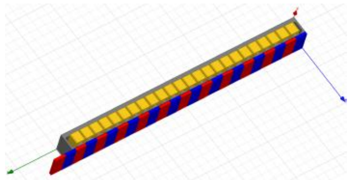

Figure 3. Full view of the all design of LBLDC

The motor was made on moving parts with supported rigid aluminum rods and linear bearings. The length of motor is equal to the length of the coils of magnets as shown in Fig. 4 is designed to function with a coil under each pole. With this configuration, the bottom of the magnets of the two remaining coils in motion without the need for any electronic circuit which energy can be obtained automatically. In addition to the energy required elimination of coils made of a single layer, increasing the number of turns required force is designed to obtain flexibility of the linear motor is provided. Ansoft Maxwell brushless direct current motor stator design is made with the program is given in Fig. 5. Laminated stator iron sheets to the packaging of 0.5 mm thickness were obtained. The moving part of the motor and the phase windings placed on the salient poles.

Placements of the magnets used in brushless DC motors are shown in Fig. 4. N and S poles of the magnets are equal dimensions placed side by side to form. The technical specifications of magnets are listed below. N42 magnets are made under Article NeFeB class; taking into account the operating temperature of the motor to operate at 150 ℃ was selected.

©2015 Engineering and Technology Publishing

Feature of magnets which are used in designing motor are; magnets sintered NdFeB N42SH Class, Br (magnetic flux density) from 1280 to 1320 mT, HCJ (in the magnetization) >= 1672kA/m, BH_max (maximum energy production): 320-343kJ/m3, Maximum Working temperature: 150

Fig. 4 shows the dimensions of the magnets and Fig. 5 shows geometric dimensions of a single stator slot used in the motor. Energize the phase windings and the motor driver board microcontroller which will speed controller is developed for the RDK-BLDC development kit Texas Instrument Company will be used.

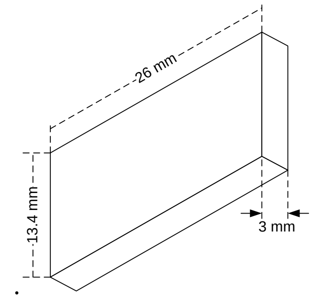

Figure 4. Dimensions of magnet and single stator slot

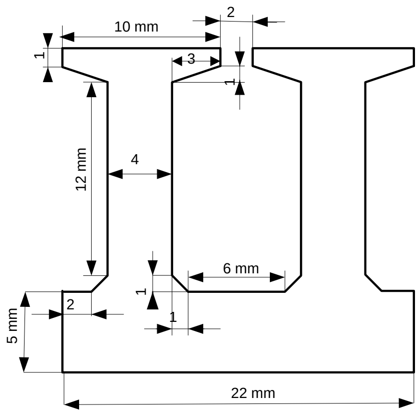

Figure 5. Dimensions of a single stator slot

Produced the force of magnets to increase the spool moving in the direction opposite to one another by means of power to the brushes and the collector is possible, if desired to the braking energy is enough to give both the same direction to the coil. Brushes are mounted in a device which can slide along with magnets. For this reason, DC linear motor can be made to desired length and does not need any drive or switching circuit.

C. Calculation of Induced Force

During the analytical analysis of electric machines is important to determine the parameters of the magnetic circuit which used for developing motor aspects of the magnetic circuit and the flux are given in Fig. 6. Current directions simultaneously energize the coils is opposite to each other, and the collector assembly is provided with a brush. It also supports the magnets, the magnetic fluxes each other condition. As shown in Fig. 6, the motor of the magnetic circuit comprises two symmetrical.

In Fig. 7, armature current is zero air magnetic flux density distribution of magnetic flux density change of the range (BgQ) Analytical and numerical analyzes of designed LBLDC were carried out on one side. According to the results of the analytical and analysis, propulsion force generated 86.0 N / A as a result of the numerical analysis of the 75.30 N / A was obtained. Analytical results come close to the simulation results show that the materials and methods consistent with the elections.

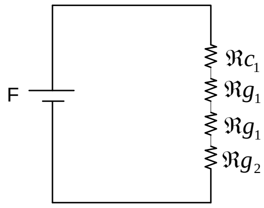

Figure 6. DC magnetic circuit of one-sided linear motor

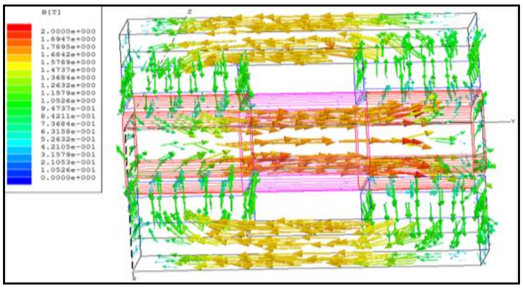

Figure 7. Magnetic flux density and vectors of LBLDC

$$\phi = B_m \times A_m = qB_g A_g \tag{2}$$

where q is the design shape and the air-gap flux leakage flux exceeds the effective coefficient is associated with the surface. Air gap equal to the beginning and end sections of materials and dimensions of the surface parallel to the active surface. This gap was calculated by calculated by Equation 3. Surfaces are not equal to each other and the Equation 4, based on small dimensions such as the surface is applied. Other than that, the different formulas for different geometric shapes can be used. Also, the calculation should be used experimentally to complex structures developed motor.

$$A_{g(a+l_g)(b+l_g)} \tag{3}$$

$A_g = 5.476\times10^{-3}$ and A_m value are 2.5×10^{-3} Surfaces are not equivalent to each other, or in the other words, the active surface leakage flux rate factor q.

Used motor magnet demagnetization curves (BH) is given in Fig. 7, the magnetic flux density Bm magnet, coercitive force Hc, Br longer magnetism, magnetic field strength magnet Hm, BQ ordinate the operating point, the operating point of the apse HQ. In the design of motor, NdFeB type magnet was used, and value of Br is 1Tesla, the value of Hc is 900^ 3 kA / m.

$$B_m = \tan\alpha H_m + B_r = \frac{B_r}{H_c} H_m + B_r \tag{4}$$

The magnetic flux density in the air gap (Bg) and magnetic field strength (Hg) as in Equation 5 is the correlation between.

$$B_g = \mu_0 H_g \tag{5}$$

Ampere's law is applied to the magnetic circuit is obtained.

$$2H_m l_m + 2H_g l_g = 0 \tag{6}$$

In equation 6, the Hg value is removed; the air gap magnetic field intensity of the expression, Equation 7 is obtained.

$$H_g = -\frac{H_m l_c}{\lg} \tag{7}$$

Also Bm values from Equation 2 is pulled out, the magnetic flux density of the magnet is found.

$$B_m = \frac{q B_g A_g}{A_m} \tag{8}$$

In Equation 8 instead of Equation 5 by writing the value Bg

$$B_g = \frac{\mu_0 q H_g A_g}{A_m} \tag{9}$$

Expression has been reached. Value obtained from Equation 7 to 9 substituting Hg can be calculated as;

$$H_g = -\frac{\mu_0 q l_m A_g}{l_g A_m} \tag{10}$$

The slope of the load line is dependent on the length of the air gap of the magnet and the magnetic circuit of the load line of the magnet longer in length upwardly, sliding up and down with increasing air gap. But the truth is demagnetization of the magnet is connected to production parameters remain constant. The intersection of two lines each operating point of the magnet is giving; Equations 5 and 10 together equalized value of the apse of the operating point is located in the Equation 11 as given.

$$H_Q = \frac{-B_r}{\frac{B_r}{H_c} + \mu_0 \frac{q A_g l_m}{A_m l_g}} \tag{11}$$

Magnetic circuit parameters in Equation 11 put in place by the magnetic field strength of the magnet operating point, H_Q = -146.102 kA /m, respectively. Instead, this value by placement in Equation 4, the operating point of the magnet magnetic flux density = 0.84 Tesla B_Q respectively. The force generated in the engine is formed in the magnetic field in the air gap, the air gap and the consideration of the cross sectional area of the magnet, the magnetic flux density in the air gap by Equation 2 respectively.

$$B_{gQ} = \frac{B_Q}{q} = 0{,}38 Tesla \tag{12}$$

Who contributed to the force generated in the motor winding two pieces of linear and L is the length of the active conductor. The two sides of each active coil are present, the total force generated in the motor with the help of Equation 12 calculated as:

$$F = 4n B_{gQ} L I \tag{13}$$

where n denotes the number of turns of the coils, with known substituting variables.

$$F = 76 I \text{ Newton} \tag{14}$$

Expression was obtained. As seen motors designed sensitivity or force / current ratio was found to be 76. This value is higher than of conventional motor is indicative of the design suitable for production.

D. *Numerical Analysis of the Magnetic Circuit and the Generated Force*

Outside the computer with the help of analytical methods in the numerical solutions of magnetic circuits are possible. In fact, this kind of work done by software, the magnetic circuit is composed of the solution of Maxwell's equations using finite element method [12]. The magnetic circuit of the motor is designed in three dimensions in Fig. 4 is drawn and simulations are carried out necessary. In this context the current through the armature windings of the motor when the magnetic circuit of the zero and the magnetic flux distribution calculated by the force generated. Fig. 6 illustrates the distribution of the magnetic circuit of the magnetic flux density. As shown in the front area of the shaft is very low magnetic flux density, a small area of the center shaft of the magnetic flux vector is around 1.8 Tesla as in Fig. 7. Half of the total magnetic flux in the upper and lower shafts, mid-shaft of the magnetic flux carried by the flux for both arms seems to be more intense. BH 1010 mild steel used in the magnetic circuit is shown in Fig. 8. Thus, on the same 1.8 Tesla coil energy will not, and the saturation magnetic flux density, will start shaft core is suitable for the selected cross-sections.

Force generated in the motor air gap has occurred, which is effective in producing the force of the air gap along the horizontal axis and the magnetic flux density change of Equation 13, as in Fig. 9 are provided BgQ . Air-gap magnetic flux density along the line, the end parts of the magnet started around 0.44 Tesla, Tesla increased to 0.68 in the middle. Outside of the magnet and the magnetic flux decreased rapidly approaching zero. Magnetic flux density over the central part of the magnet decrease towards to the ends. When you go out of the magnetic flux density of the magnet observed a rapid decline.

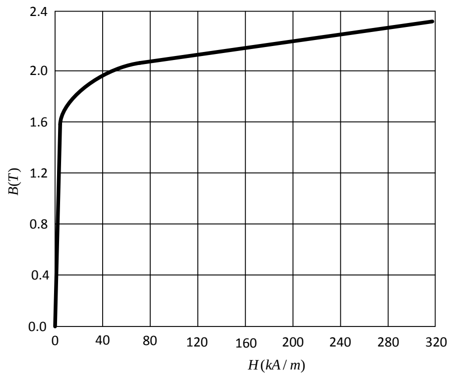

Figure 8. B-H curve of 1010 steel.

E. Mathematical Model of LBLDC

In the three phased BLDC motor and Induction Motor systems, instead of the three phases, simplified two phased d-q mathematical model has been using as a widely. In Table I, sensor and switching situations was given. Also, showed in Fig. 9, the derivation of LBLDC from BLDC. In the study the dynamic behavior of the dq axis transformation is LBLDC simplifies the mathematical expressions. LBLDC mathematical expressions, circular BLDC two-axis dq model by making the necessary transformation of Equation (15) are also given. These transformations Clarke Transformation: abc α-β axis of the axis system transformation system can be written as.

$$\begin{bmatrix} S_\alpha \\ S_\beta \end{bmatrix} = \frac{2}{3}\begin{bmatrix} 1 & -\frac{1}{2} & -\frac{1}{2} \\ 0 & \frac{\sqrt{3}}{2} & -\frac{\sqrt{3}}{2} \end{bmatrix}\begin{bmatrix} S_a \\ S_b \\ S_c \end{bmatrix} \tag{15}$$

The park transformation is α-β transformation of the axis system to the dq axis system;

$$\begin{bmatrix} S_d \\ S_q \end{bmatrix} = \begin{bmatrix} \cos\theta & \sin\theta \\ -\sin\theta & \cos\theta \end{bmatrix}\begin{bmatrix} S_\alpha \\ S\beta \end{bmatrix} \tag{16}$$

where S is a current, voltage and the magnetic flux vectors represents of BLDC. The moving part in the first side LBLDC energy (magnetic field occurring in the windings of the moving area) where the stationary part of the permanent magnet, which is superimposed a linear movement occurs. In Table I was given motor sensor's and switching situations.

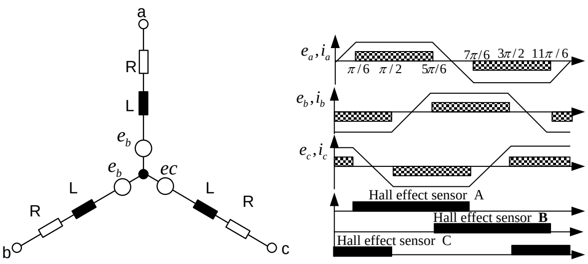

Figure 9. The derivation of LBLDC from BLDC [10].

TABLE I. SENSOR AND SWITCHING SITUATIONS

Stage	1	2	3	4	5	6
Sensor A						
Sensor B						
Sensor C						
Code	100	101	001	011	010	110
	clockwise					
Sensor A	-	0	+	+	0	-
Sensor B	+	+	0	-	-	0
Sens ör C	0	-	-	0	+	+
	counterclockwise					
Sensor A	+	0	-	-	0	+
Sensor B	-	-	0	+	+	0
Sensor C	0	+	+	0	-	-

In this study, BLDC's when forming the magnetic circuit mathematical expressions is assumed to be linear. This acceptance dq equivalent circuit given in Fig. 10 from the three-phase resistance and inductance of the first side was considered dq axis voltage equations in mathematical expressions can be write as in Eq 17 and Eq 18 as:

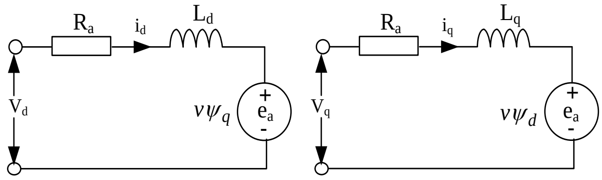

Figure 10. The equivalent circuit at d-q axis of LBLDC

$$V_d = Ri_d + L_d\frac{di_d}{dt} - \frac{\pi}{\tau}vL_q i_q \tag{17}$$

$$V_d = Ri_q + L_q\frac{di_q}{dt} - \frac{\pi}{\tau}v(L_d i_d + \psi_f) \tag{18}$$

If magnetic flux equations by Equation 19 and Equation 6 can be write as:

$$\psi_d = L_d i_d + \psi_f \tag{19}$$

$$\psi_q = L_q i_q \tag{20}$$

Electromagnetic repulsion force;

$$F_i = \frac{3}{2}\frac{\pi}{\tau}\left[\psi_f + \left(L_d - L_q\right)\times i_d\right]i_q \tag{21}$$

If Id = 0 is taken as if the electromagnetic repulsion force is calculated by Equation (22).

$$F_i = \frac{3}{2}\frac{\pi}{\tau}\psi_f i_q \tag{22}$$

Considering the mechanical load of the electromagnetic repulsion force is calculated by equations (23) and the velocity is calculated by Equation (24).

$$F_i = F_d + B\upsilon + M\frac{d\upsilon}{dt} \tag{23}$$

$$\upsilon = 2.f.\tau \tag{24}$$

Thus LBLDC mathematical expressions used in the control is obtained. Where ψf is the permanent magnet flux, the external force Fd applied externally, B friction coefficient, M is the weight of the movable member, the movable member speed, the phase winding resistance R, the frequency f, τ is the terminal step.

TABLE II. SHEET CUTTING MEASURES OF CORE PACKAGES POSTURE

Units	Sizes
Core packet size	340 mm
Core width	40 mm
Thickness of metal sheet	46 mm
Slot depth	15 mm
Slot width	7 mm
Tooth width	7 mm
Tooth width of head part	5.5 mm

©2015 Engineering and Technology Publishing

LBLDC in this study for the first aspect in the design of electrical steel sheet with a thickness of 0.3 mm was used. A first side of the core prepared in the used sheet size is given in Table II.

Brushless circular machine to obtain the rotating magnetic field is sufficient to at least two phase windings. Similarly to obtain walking area of the at least three phase windings are required. Identical three-phase windings to create walking space between the winding flux axis 2τ / place of 120º difference and phase difference between winding stream should be. An LBLDC shape for a plurality of coils has been proposed [10]. Here coveted and frequently used in practice is used and the winding shape, the winding form is given Fig. 11.

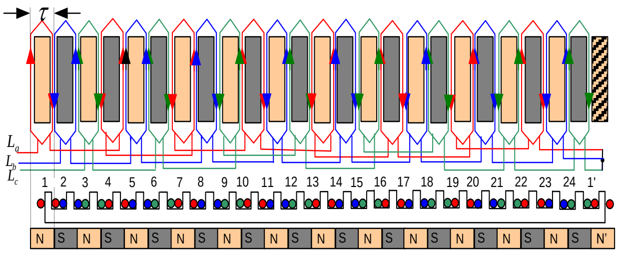

Figure 11. The single-layer winding arrangement and placement of the magnets.

When creating the first side winding of the motor intended to be 3-phase 8-pole , 0.35 mm diameter copper wire is used and each slot 220 so that SIP winding was performed .Second side, as in Fig. 11 on the soft iron plates are arranged to be surface magnets. Type magnet used in this study, according to the magnetic flux density greater than other varieties neodymium (NdFeB) magnets are [1]. This study used the measuring neodymium magnets are given in Table II. Neodymium magnet dimensions are length 40 mm, and thickness 10 mm, width 20 mm. The first side was measured as the R value 1.6 Ω. Measurements made with an LCR meter, the RAB = 2.3 Ω, RAC = 2.3 Ω, RBC = 2.28 Ω respectively. R value from the results of this measurement was taken as 1.6 Ω. Fig. 12 shows that the motor magnets of the aluminum track shape arrayed and Fig. 13 shows the winding connections of the motor side view and Fig. 14 shows winding connections of the motor mounted bottom view. Complete experiment set of LBLDC was given in Fig. 15 and Fig. 16 and Fig. 17 motor phase resistance and inductance measuring respectively.

Determination of the side inductance (L) in the locked state current is applied at frequencies of 5 Hz and 10 Hz. IK obtained in these experiments (Locked first side stream) and VK (Locked first side voltage) level , the motor was calculated XL.

Superficial variable reluctance force magnet synchronous motor to be zero, d and q axis inductance value of L is calculated equal to each other , and 2/3 is known to be equal to [10]. By means of this data is determined as L value 1.83 mH.

Made with LCR meter to measure, LAB = 3.86 mH, LAC = 3.86 mH LBC = 3.86 mH, respectively. L value from the results of this measurement is calculated 0.183 mH.

F. Determination of the Magnetic Flux in the Air Gap

Calculation of the value of the magnetic flux of the permanent magnet 12 is calculated parameter value using Equation [25]. Calculations made, ψf = 0.183 Wb was obtained by this equation:

$$\psi_f = \frac{2}{\pi} \tau N.B_f l_1 k_{w1} \tag{25}$$

where N is the number of turns in a phase, l1 is the length of side sheets stack packages, Bf = 0.7 T magnetic flux density shows the winding factor kw1=1 [2]. The parameters of the motor are given in Table III.

Figure 12. The motor magnets of the aluminum track shape arrayed

TABLE III. THE PARAMETERS OF LBLDC

Units	Symbols	Values
Poles numbers	p	24
Primary side resistance	R	1.6 Ω
Magnet flux	ψf	0.183 Wb
d axis inductance	Ld	28 mH
q axis inductance	Lq	28 mH
Phase voltage	V	24 V
Phase Current	I	3.0 A
Pole pitch	τ	0.042 m
Motor weight	m	1.6 kg
Frequency	f	15 Hz

Figure 13. The winding connections of the motor side

Figure 14. Winding connections of the motor mounted bottom side

Figure 15. Complete experiment set of LBLDC

©2015 Engineering and Technology Publishing

Figure 16. Measurement of phase inductance of LBLDC

Figure 17. Measurement of phase resistance of LBLDC

III. CONCLUSION

In this study a single-sided LBLDC was simulated as analytical and a prototype released. Released motor tested and parameters were measured. The designed motor has 3 A, 24 V, 72 W, and 70 N pull force, high force/volume rated and low cost. Its characteristics were analyzed by using finite-element software. The characteristics of motor were analyzed by using finite-element software. The obtained results were compared with the results obtained by the analytical methods.

ACKNOWLEDGMENT

This study has founded by the Scientific Research Fund project was supported by Gazi University as 49/2011-03 coded

REFERENCES

[1] J. T. Griffiths and P. L. Jones, "The direct current linear motor and its applications," in *Proc. Universities Power Engineering Conference*, Nottingham University, England, 1969, pp. 89-91.

[2] C. W. Gren and R. J. Paul, "Performance of DC linear machines based on an assessment of flux distributions," in *Proc. the Institution of Electrical Engineers*, vol. 118, no. 10, 1971, pp. 1413-1420.

[3] A. Basak and K. J. Overshott, "The ferrite field DC linear motor," in *Proc. IEE Conference on Linear Electric Machines*, IEE Publication, vol. 120, 1974, pp. 39-44.

[4] S. A. Nasar and I. Boldea, *Linear Electric Motors: Theory, Design, and Practical Applications*, America: Prentice-Hall, 1987, pp. 4-23.

[5] A. Basak and F. J. Anayi, "A DC linear motor with a square armature," *IEEE Trans on Energy Conversion*, vol. 10, no. 3, pp. 462-469, 1993.

[6] W. Kim and B. C. Murphy, "Development of a novel direct-drive tubular linear brushless permanent-magnet motor," *International Journal of Control, Automation, and Systems*, vol. 2, no. 3, pp. 279-288, 2004.

[7] R. C. Okongwo and R. Hanitsch, "Development and control of a prototype permanent-magnet dc linear motor," *IET Electr. Power Appl.*, vol. 1, no. 2, pp. 223-238, 2007.

[8] M. Nasri, H. Nezamabadi-pour, and M. Maghfoori, "A PSO-based optimum design of PID controller for a linear brushless DC motor," in *Proc. World Academy of Science: Engineering & Technolog*, vol. 20, 2007, pp. 211.

[9] J. K. Kim, S. W. Joo, S. C. Hahn, and J. P. Hong, "Static characteristics of linear BLDC motor using equivalent magnetic circuit and finite element method," *IEEE Transactions on Magnetics*, vol. 40, no. 2, pp. 742–745, March 2004.

[10] P. Damodharan and K. Vasudevan, "Sensorless brushless DC motor drive based on the zero-crossing detection of back electromotive force (EMF) from the line voltage difference," *IEEE Transactions on Energy Conversion*, vol. 25, no. 3, pp. 661-668, 2010.

Mahir Dursun was born in 1970, Corum, Turkey. He received the BS degree in 1993, the MSc degree in 1996, and the PhD degree 2002 from Gazi University, Ankara, Turkey. He is currently an associate professor at the Department of Electric Machinery Education, Gazi University. His research interests include, Motor Design, Modeling, Motor Control, Switched Reluctance Motors, Linear Switched Reluctance Motors, Brushless DC motors, DC-DC converters, Matrix Converters, FLC, Artificial Neural Network, Elevator motors, Motor and Centrifugal Pump Drivers, DSP, PLC, microprocessors and microcontroller programming, serial and parallel active power filters, and photovoltaic systems, photovoltaic irrigating systems, RF control and communications, and distance education material design..

Ali Saygın was born in Sivas, Turkey in 1974. He graduated from the Department of Electrical Education of Gazi University in 1995. He received the M.Sc. and Ph.D. degree from the Institute of Science and Technology of Gazi University in 1998 and 2004 in Electrical Education from Technical Education Faculty. His general research interests are in control systems, analysis and simulation of electrical machines, and motion control

Semih Ozden was born in 1982, Aydın, Turkey. He received the BS degree in 2004, the MSc degree in 2007 and PhD in 2013 from Gazi University, Ankara, Turkey. He works at Gazi University, OSTIM Vocational School as lecturer. His research interests include photovoltaic systems, photovoltaic irrigating systems, switched reluctance motors, linear switched reluctance motors, motor control and controllers. Also he has publication about machine learning application on smart systems with experimentally.

Ahmet Fenercioğlu received B.Sc. and M.Sc. degree in Department of Electrical Education from Marmara University, Istanbul, Turkey in 1994 and Ph.D. degree in Electrical Machinery from Gazi University, Ankara, Turkey in 2006. He has worked as an instructor in Department of Mechatronics Education in Gaziosmanpasa University, Tokat, Turkey. He has studied design of electrical machinery.

©2015 Engineering and Technology Publishing